Animal Microbiome

RESEARCH Open Access

Dietary regulation on gut resistome linked with microbial amino acid metabolism in pigs

Ziyu Liu[1,2†], Chengming Meng[1,2†], Junhua Shen[1,2], Huisong Wang[1,2], Jiaqing Guo[1,2], Jiangchao Zhao[3], Chunlong Mu[1,2,4*] and Weiyun Zhu[1,2,5*]

Abstract

Dietary protein plays a crucial role in shaping the gut microbiome and modulating intestinal amino acid metabolism. Gut microbiome is recognized as a reservoir for carrying antimicrobial resistance genes. However, the relationship between amino acids metabolism and antibiotic resistome remains poorly understood. Here, a pig model was used to study this relationship by comparing the impact of dietary casein hydrolysate diet with those of an intact casein diet. Metabolomics analysis revealed that casein hydrolysate supplementation primarily altered amino acid metabolism, characterized by significantly reduced levels of several amino acids, including tyrosine and glutamine, accompanied by increased levels of amino acid–derived metabolites. Metagenomics analyses indicated that these metabolic shifts were closely associated with microbial changes in the gut, particularly the genera *Escherichia* and *Bifidobacterium*. Consistently, microbial genes related to amino acid transport and metabolism exhibited higher abundances. Notably, the abundances of antibiotic resistance genes (ARGs) and mobile genetic elements (MGEs) were significantly enriched in response to casein hydrolysate supplementation. Integrated metabolome–resistome correlation analyses revealed significant associations between multiple amino acids, including tyrosine and glutamine, and distinct ARG subtypes, indicating a tight coupling between amino acid metabolism and antibiotic resistance potential. Metagenomics binning and assembly further resolved the taxonomic origins of these functional traits. Specifically, in *Escherichia fergusonii* and *Bifidobacterium thermophilum*, genes related to amino acid metabolism, ARGs, and MGEs were co-localized on the same contigs with close genomic proximity. Together, these findings highlight a strong link between microbial amino acid metabolism and the resistome, suggesting that dietary casein hydrolysate reshapes both microbial metabolic functions and antibiotic resistance potential within the intestinal ecosystem.

Keywords Casein hydrolysate, Gut microbiome, Amino acids, Resistome, Metagenomics

†Ziyu Liu and Chengming Meng contributed equally to this work.

*Correspondence:
Chunlong Mu
chunlong.mu1@ucalgary.ca
Weiyun Zhu
zhuweiyun@njau.edu.cn
[1]Laboratory of Gastrointestinal Microbiology, College of Animal Science and Technology, Nanjing, China
[2]National Center for International Research on Animal Gut Nutrition, Nanjing Agricultural University, Nanjing, Jiangsu, China
[3]Department of Animal Science, University of Arkansas, Fayetteville, AR, USA
[4]Present address: Department of Microbiology, Immunology, and Infectious Diseases, Cumming School of Medicine, University of Calgary, Calgary, Canada
[5]State Key Laboratory of Meat Quality Control and Cultured Meat Development, Nanjing Agricultural University, Nanjing, Jiangsu, China

Introduction

Different forms of dietary protein, including intact proteins and protein hydrolysates, can differentially influence gut health by shaping microbial community composition, modulating metabolic activity, and affecting host–microbe interactions [1, 2]. Casein hydrolysate, which is enriched in peptide-bound amino acids and bioactive peptides, has been proposed as a nutritional intervention to improve gut function and metabolic homeostasis, potentially conferring advantages over intact casein. Previous studies have shown that dietary casein hydrolysate accelerates gastric transit [3], promotes enteroendocrine cell development [4], and facilitates the colonization of *Lactobacillus amylovorus* in the small intestine [5]. More recent evidence further indicates that casein hydrolysate regulates epithelial amino acid and peptide transport, as well as gastric acid secretion [6]. Despite these advances, how casein hydrolysate influences microbial amino acid metabolism within the gut ecosystem remains poorly understood.

Microbial transport and metabolism of amino acids are central to the functioning of the gut ecosystem [7]. Beyond serving as energy sources for microbial growth, amino acids in the intestinal lumen also serve as precursors to a wide array of metabolites that influence gut health and host physiology [8]. For example, microbial amino acid metabolism can generate neuroactive compounds, underscoring the functional connections between the gut microbiota and the gut–brain axis [9]. In addition to these host-oriented effects, accumulating evidence suggests that microbial amino acid metabolism is also closely associated with the expression and distribution of antimicrobial resistance genes.

The resistome refers to the complete collection of antibiotic resistance genes (ARGs) within a microbial community, encompassing genes harbored by both pathogenic and non-pathogenic microorganisms [10]. These genes may be intrinsic, being naturally encoded in specific bacterial species, or acquired through mutation and horizontal gene transfer [11]. ARGs encode diverse mechanisms that enable bacteria to withstand antibiotic exposure, including drug inactivation, modification of antibiotic target sites, and active efflux of antimicrobial compounds. Although ARGs are widely distributed across the gut microbiome and may not pose an immediate clinical threat, they represent a substantial reservoir with the potential to contribute to antimicrobial resistance through selective pressures or gene transfer events [12, 13]. Functionally, ARGs encode a broad range of resistance strategies, such as enzymatic degradation of antibiotics, efflux pump systems, and target modification, and are frequently associated with mobile genetic elements (MGEs) that facilitate their mobilization and dissemination within microbial communities [14–16]. While ARGs have traditionally been studied in the context of antibiotic exposure, growing evidence indicates that non-antibiotic factors—including nutrient availability and microbial metabolic activity—can also influence their abundance and persistence [17, 18]. For instance, arginine limitation has been shown to induce a tolerant physiological state in *Staphylococcus aureus*, thereby reducing susceptibility to antibiotics [19]. Conversely, bacterial metabolites such as amino acids and nucleotides can enhance cellular metabolic activity, resensitize tolerant bacterial populations, and improve antibiotic efficacy [20]. Collectively, these findings highlight amino acid transport and metabolism as emerging modulators of resistance dynamics within the gut microbiome.

In this study, pigs fed diets containing either casein hydrolysate or intact casein were used as a model to investigate the dietary regulation of intestinal amino acid metabolism and the resistome. By integrating metagenomics and metabolomics analyses, we characterized microbial responses in amino acid transport and metabolic pathways following casein hydrolysate supplementation. Given the pronounced differences in both dietary amino acid composition and cecal amino acid profiles, corresponding changes in ARGs and MGEs were further examined. Together, these analyses aimed to clarify how dietary casein hydrolysate modulates microbial metabolism and antimicrobial resistance potential, providing new insights into the interplay among amino acids, the gut microbiome, and the resistome.

Materials and methods

Animal experimental design and sample collection

All animal care and experimental procedures were carried out in full compliance with the ethical guidelines approved by the Animal Care and Use Committee of Nanjing Agricultural University (Approval No. SYXK (Su) 2017-0007). The primary objective of this study was to investigate the biological effects of different dietary protein forms, specifically intact casein versus casein hydrolysate. The trial was conducted at the research facilities of the College of Animal Science and Technology, Nanjing Agricultural University. A total of 16 Duroc × Landrace × Yorkshire crossbred barrows (63 ± 2 days old) with an average initial body weight of 19.09 ± 0.61 kg were randomly allocated to two dietary treatments (n = 8 per group): intact casein supplementation (IC) and hydrolyzed casein supplementation (HC), as described in our previous study [3]. The composition and nutritional profiles of experimental diets are detailed in Table S1. To maintain dietary balance, pigs received 85% of the standard feed amount, distributed equally over three daily feeding sessions, and had ad libitum access to water throughout the study. The ambient temperature of the pig house was maintained at 24 ± 2 °C. The feeding trial

lasted for 28 days, during which animal health and well-being were closely monitored. Routine ventilation and cleaning were performed to maintain hygienic housing conditions. Daily observations included feed intake, fecal consistency, and general behavior to assess overall health status. At the end of the experiment on day 29, all pigs were anesthetized with an intravenous injection of 4% sodium pentobarbital solution (40 mg/kg body weight) and euthanized by exsanguination. Cecal digesta samples were aseptically collected, immediately transferred into sterile cryotubes, snap-frozen in liquid nitrogen, and stored at − 80 °C until further analysis.

Metagenomics sequencing

Microbial genomic DNA was extracted from cecal digesta samples using the E.Z.N.A.® Stool DNA Kit (Omega Bio-Tek, USA), following the manufacturer's instructions. DNA quality and integrity were assessed via 1% agarose gel electrophoresis. Subsequently, 1 μg of DNA per sample was fragmented using a Covaris S220 ultrasonicator (Woburn, MA, USA). DNA library preparation was performed using a commercially available protocol (Biozeron, China), and sequencing was carried out on the Illumina HiSeq X platform with 150 bp paired-end reads. Raw reads were subjected to quality control procedures to eliminate sequencing adapters and low-quality bases using Trimmomatic (v0.36) with parameters (ILLUMINACLIP: adapters.fa:2:30:10 SLIDINGWINDOW:4:15 MINLEN:75) [21]. To eliminate host-derived sequences, the clean reads were aligned to the Sus scrofa reference genome (Sscrofa11.1, Ensembl release 104) using bowtie2 software (v2.5.4). In addition, quality-controlled reads were aligned against the human reference genome (hg19) and PhiX174 genome using Bowtie2 with default parameters, and reads mapping to these references were removed prior to downstream analyses. Taxonomic classification of the host-removed reads was performed using Kraken2 (v2.0.6) with the following parameters (--threads 16 --quick --report-zero-counts --gzip-compressed --paired). Then, assembly of the host-removed reads was conducted using MEGAHIT (v1.1.1-2-g02102e1) with the parameter (--min-contig-len 500). Open reading frames (ORFs) were predicted from assembled contigs using Prodigal [22]. Redundant ORFs were clustered into a non-redundant gene catalog using CD-HIT (v4.8.1) with stringent parameters (-n 9 -c 0.95 -G 0 -M 0 -d 0 -aS 0.9 -r 0 -T 40) [23]. Quantification of gene abundance was performed using Salmon software (v1.1.0) [24].

Taxonomic annotation of the non-redundant gene set was performed using DIAMOND (v0.9.22.123) in BLASTP mode against the NCBI non-redundant (NR) protein database. KEGG annotation was performed using KofamScan (v1.2.0), which assigns KO terms to predicted genes based on HMM profiles in the KEGG database. Based on the taxonomic classifications derived from the NR database, alpha diversity indices (Shannon and Simpson) and beta diversity distances (Jaccard) were computed using the vegan package in R (v4.3.1).

Nontargeted metabolomics

Approximately 100 mg frozen cecal digesta was cryopulverized with liquid nitrogen and extracted in 80% methanol (0.1% formic acid). After vortexing and incubating on ice for 5 min, samples were centrifuged at 15,000 ×g, 4 °C, for 5 min. The supernatant was diluted to 53% methanol with LC-MS grade water, transferred to clean tubes, and centrifuged again under the same conditions for 10 min. Final supernatants were used for LC-MS/MS.

Metabolites were analyzed using a Vanquish UHPLC coupled to a Q Exactive™ HF Orbitrap MS (Thermo Fisher) with a Hypersil GOLD C18 column (100 × 2.1 mm, 1.9 μm) at 0.2 mL/min. The 17-minute gradient was: 2% B (0–1.5 min), 2–100% B (1.5–12.0 min), 100% B (12.0–14.0 min), 100–2% B (14.1–14.9 min), and 2% B (14.9–17.0 min). Mobile phases were 0.1% formic acid in water (A) and methanol (B) for positive mode; 5 mM ammonium acetate (pH 9.0) replaced A in negative mode. MS conditions: spray voltage 3.2 kV, capillary temperature 320 °C, sheath gas 40, auxiliary gas 10.

Data were processed with Compound Discoverer 3.1 for feature extraction, alignment, and quantification (mass tolerance 5 ppm, RT tolerance 0.2 min, peak intensity ≥ 100,000, $S/N \geq 3$). Intensities were normalized to total ion current, and metabolites were identified using mzCloud, mzVault, and MassList, with annotations from KEGG (https://www.genome.jp/kegg), HMDB (https://hmdb.ca), and LIPID MAPS (https://www.lipidmaps.org).

Measurement of short-chain fatty acids and organic acids

Short-chain fatty acids (SCFAs) in cecal digesta were analyzed following a protocol established in our laboratory [5]. The concentrations of formic acid, lactic acid, and succinic acid in cecal digesta were determined using a high-performance liquid chromatography system (Thermo Fisher Scientific, USA). For standard curves, 20 mg each of lactic, formic, and succinic acids were dissolved in 1 mL double-distilled water to prepare stock solutions, which were then serially diluted 2–20 fold and filtered (0.22 μm). For samples, ~ 0.5 g digesta was suspended in 1.5 mL water, vortexed, and centrifuged at 12,000 rpm for 10 min. One milliliter of supernatant was mixed with 200 μL of 25% metaphosphoric acid and stored at − 20 °C overnight. After thawing, it was centrifuged twice (12,000 rpm, 15 min each), filtered (0.22 μm), and analyzed by HPLC. Acid concentrations were calculated using standard curves.

Identification of ARGs and MGEs

ARGs were identified using the ARGs-OAP (v 3.2.4) pipeline with the default settings based on host-removed reads in FASTQ format. The mobileOG-db (v2.0) was downloaded and used to build the MGE database. MGEs were identified by aligning ORFs files to the mobileOG database using DIAMOND with the following parameters (--evalue 1e-10 --id 90 --max-target-seqs 70). The number of prokaryotic cells in each sample was estimated by ARGs-OAP, and MGE abundance was subsequently normalized to copies per cell accordingly.

MAG binning, taxonomic classification and functional annotation

High-quality metagenome assemblies were generated from host-removed reads using MetaSPAdes (v3.14.0) with default parameters. Contigs from each sample were subsequently binned into metagenome-assembled genomes (MAGs) using the MetaWRAP pipeline, which integrates three binning algorithms: MetaBAT2, MaxBin2, and CONCOCT. MAGs with >70% completeness and <5% contamination were retained for downstream analysis. Following bin refinement, dereplication was performed between samples using dRep (v3.5.0) with parameters (-sa 0.9 -pa 0.85), and genome quality was assessed using the lineage_wf method in CheckM. Taxonomic classification of dereplicated MAGs was conducted using GTDB-Tk (v2.3.2) against the GTDB reference database (release R214).

ORFs were predicted from dereplicated MAGs using Prodigal in metagenomics mode. A phylogenetic tree was constructed using PhyloPhlAn (v3.1.68) under high-diversity settings. Functional annotation of MAG-derived ORFs was performed using multiple databases: KEGG orthologs were assigned using KOfamKOALA (exec_annotation); ARGs were identified via DIAMOND against the CARD database (--evalue 1e-7 --id 80 --max-target-seqs 70); and MGEs were annotated by aligning against the mobileOG database with DIAMOND as previously described.

Statistical analysis and visualization

All data were analyzed and visualized in R. Concentrations of targeted organic acids and selected microbial genes were analyzed using non-parametric statistical tests due to their non-normal distribution. For comparisons between two groups, the Mann–Whitney U test was applied. Differences were considered statistically significant at $P < 0.05$.

Metabolomics data were analyzed using the limma package after log2 transformation of metabolite abundances. *P* values were adjusted for multiple testing using the Benjamini–Hochberg method. Differential metabolites were defined as those with false discovery rate (FDR) ≤ 0.10 and |log2 fold change| ≥ 1, with VIP ≥ 1 from OPLS-DA used for feature prioritization. In addition, metabolites with nominal $P < 0.05$ and $0.10 < \text{FDR} \leq 0.25$ were considered as potential (trend-level) changes.

KEGG pathway enrichment was performed using a rank-based GSEA approach (fgsea) based on KEGG compound IDs and limma-derived statistics, and pathway-level significance was assessed using FDR-corrected *P* values. Furthermore, increased and decreased metabolites were analyzed separately for pathway enrichment using MetaboAnalyst to identify direction-specific metabolic alterations.

Associations between microbial features and metabolites were explored using a sparse partial least squares (sPLS) regression framework implemented in the mixOmics R package. The correlation network was constructed using the Spearman method and the igraph package in R.

Differential abundance analysis of ARGs and MGEs was performed using MaAsLin2. Associations between ARG/MGE features and experimental groups were modeled using multivariable linear models with appropriate normalization and transformation, and features with an FDR < 0.05 were considered significantly different. R^2 and *P* values for beta diversity were calculated using PERMANOVA with the adonis2 function in the vegan R package. To evaluate the global concordance between metabolomics profiles and antibiotic resistance–related features, Procrustes analysis was performed based on ordination results derived from each dataset. Associations between different data matrices were further quantified using Mantel tests, whereas feature-level associations between individual metabolites and ARG gene abundances were assessed using Spearman's rank correlation analysis.

The phylogenetic tree was visualized using iTOL (https://itol.embl.de). Gene clusters were visualized using the ChiPlot online platform (https://www.chiplot.online).

Results

Casein hydrolysate reshaped the cecal metabolome with pronounced effects on amino acid metabolism

To investigate the effects of casein hydrolysate on cecal metabolic profiles, we performed untargeted metabolomics analysis. Orthogonal partial least squares discriminant analysis (OPLS-DA) demonstrated a clear separation between IC and HC groups, indicating overall metabolic signatures following casein hydrolysate supplementation (Fig. 1A).

To characterize pathway-level metabolic alterations without pre-selecting differential metabolites, KEGG pathway enrichment analysis was conducted using fgsea based on ranked global metabolite changes between the IC and HC groups. This analysis revealed significant

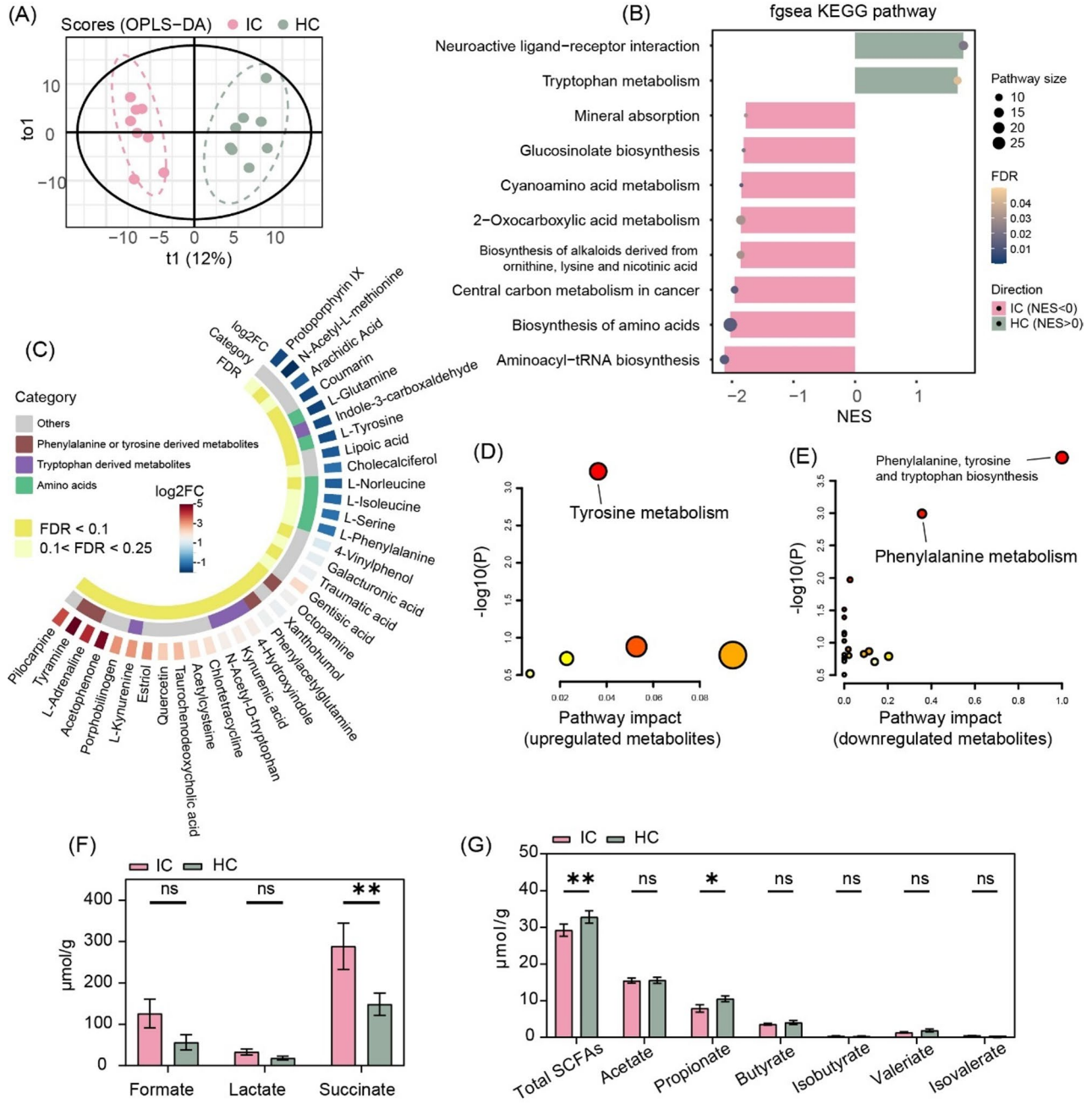

Fig. 1 Metabolomics profiling and metabolites differences between IC and HC groups. (**A**) OPLS-DA score plot showing the separation of samples between groups. (**B**) KEGG pathway enrichment analysis using fgsea based on global metabolite changes. The normalized enrichment score (NES) indicates pathways enriched in IC (NES < 0, pink) or HC (NES > 0, green). Dot size represents the number of metabolites contributing to pathway enrichment, and color represents FDR-adjusted *P* values. (**C**) Circular heatmap of differential metabolites between IC and HC groups. Metabolites are grouped by biochemical categories. Differential metabolites were defined as those with FDR < 0.1, |log2 FC| ≥ 1, and VIP ≥ 1. Metabolites with 0.1 ≤ FDR < 0.25 were considered as potential (trend-level) changes. The outer ring indicates log2 FC, and the inner ring denotes statistical significance. Pathway impact analysis of upregulated (**D**) and downregulated (**E**) metabolites. (**F**) Barplot showing cconcentrations of formate, lactate, and succinate. (**G**) Barplot showing concentrations of total and individual short-chain fatty acids (SCFAs)

enrichment of multiple amino acid–related pathways, including amino acid biosynthesis, aminoacyl-tRNA biosynthesis, and tryptophan metabolism, with clear directional enrichment patterns between groups (Fig. 1B).

Subsequently, differential metabolite analysis identified a set of metabolites showing significant or trend-level changes between groups. Based on combined criteria of FDR < 0.1, $|\log_2 FC| \geq 1$, and VIP ≥ 1, metabolites were defined as significantly altered, whereas metabolites

with $0.1 \leq FDR < 0.25$ were considered potential changes. These discriminative metabolites were mainly involved in amino acid metabolism and their downstream derivatives. Specifically, several amino acids, such as tyrosine and glutamine, were significantly decreased in the HC group, whereas aromatic amino acid–derived metabolites, including kynurenine, tyramine, and adrenaline, were markedly increased (Fig. 1C).

To further elucidate the pathways driving these metabolite-level changes, pathway topology analysis was performed separately for upregulated and downregulated metabolites (Fig. 1D and E). Metabolites elevated in the HC group were primarily mapped to tyrosine metabolism ($FDR < 0.05$), which emerged as the most impacted pathway, whereas metabolites reduced in the HC group were mainly associated with phenylalanine metabolism and phenylalanine, tyrosine, and tryptophan biosynthesis pathways ($FDR < 0.05$).

In addition to amino acid–related alterations, quantitative analysis of organic acids revealed a significant decrease in succinate concentrations in the HC group, while formate and lactate levels remained unchanged (Fig. 1F). Moreover, the total concentration of short-chain fatty acids (SCFAs) was significantly higher in the HC group, mainly attributable to elevated propionate levels (Fig. 1G). Collectively, these results demonstrate that casein hydrolysate supplementation markedly reshapes the cecal metabolic environment, with pronounced effects on amino acid metabolism and downstream fermentation outputs.

Altered amino acid profile is associated with microbial genera and metagenome-encoded transport and metabolic functions

Given the alterations in amino acid profiles observed in the cecal metabolome, we next examined whether these changes were associated with variations in gut microbiota composition and microbial functional potential. Based on the metabolomics results, we focused on a set of amino acids and related metabolites that exhibited pronounced alterations, including glutamine, serine, tyrosine, isoleucine, and phenylalanine, and examined whether variation in gut microbiota could collectively explain these changes. To this end, sparse partial least squares (sPLS) analysis was applied to relate the selected metabolites to genus-level microbial profiles.

Within this framework, the sPLS model identified bacterial genera whose loadings on the first component best explained the covariation between microbial composition and the selected amino acid features, highlighting taxa most strongly associated with the altered amino acid landscape (Fig. 2A and B). Genera displaying loading directions opposite to those of amino acids, such as *Escherichia*, were negatively associated with these metabolites, whereas genera sharing the same loading direction, including *Bifidobacterium* and *Megasphaera*, were positively associated. To further delineate the direction and strength of these associations, a correlation network was constructed based on the sPLS-selected metabolites and genera, enabling visualization of positive and negative genus–amino acid relationships (Fig. 2C).

To further explore whether the microbiota-associated amino acid alterations were accompanied by changes in microbial functional capacity, we examined metagenome-derived KEGG-annotated genes involved in amino acid transport and metabolism. In this pathway analysis, we primarily focused on microbial transport of amino acids and their subsequent metabolism into succinate and propionate, which were markedly altered following casein hydrolysate supplementation (Fig. 2D).

The general L-amino acid transporter system—including K09969 (*aapJ*, substrate-binding protein), K09970 (*aaQ*, permease protein), K09971 (*aaM*, permease protein), and K09972 (*aaP*, ATP-binding protein)—was significantly more abundant in the HC group, suggesting an increased microbial capacity for amino acid uptake. In parallel, several enzymes involved in amino acid metabolism were also enriched in the HC group. These included key enzymes related to tyrosine and phenylalanine metabolism—such as K00813 (*aspC*, aspartate aminotransferase) and K00832 (*tyrB*, aromatic amino acid transaminase)—as well as enzymes associated with isoleucine metabolism, including K01825 (*fadB*, 3-hydroxyacyl-CoA dehydrogenase) and K00632 (*fadA*, acetyl-CoA acyltransferase). In addition, genes associated with the tricarboxylic acid (TCA) cycle showed significantly higher abundance in the HC group. Notably, these included K00242 (*sdhD*, succinate dehydrogenase subunit) and K00164 (*OGDH*, 2-oxoglutarate dehydrogenase E1 component). Furthermore, the HC group exhibited increased abundance of regulatory genes involved in succinate and propionate transport. These included K07701 (*dcuS*, sensor histidine kinase DcuS), K07703 (*dcuR*, response regulator DcuR), K07710 (*atoS*, sensor histidine kinase AtoS), and K07714 (*atoC*, response regulator AtoC). Overall, these results demonstrate that alterations in several key amino acids are closely associated with gut microbiota and occur in parallel with changes in metagenome-encoded functions related to amino acid transport, metabolism, and downstream fermentation pathways following hydrolyzed casein supplementation.

Casein hydrolysate modulated antibiotic resistance genes and mobile genetic elements

To evaluate the impact of casein hydrolysate on microbial antibiotic resistance potential, ARGs were profiled using the ARGs-OAP pipeline, based on host-depleted metagenome reads. Alpha diversity analysis revealed

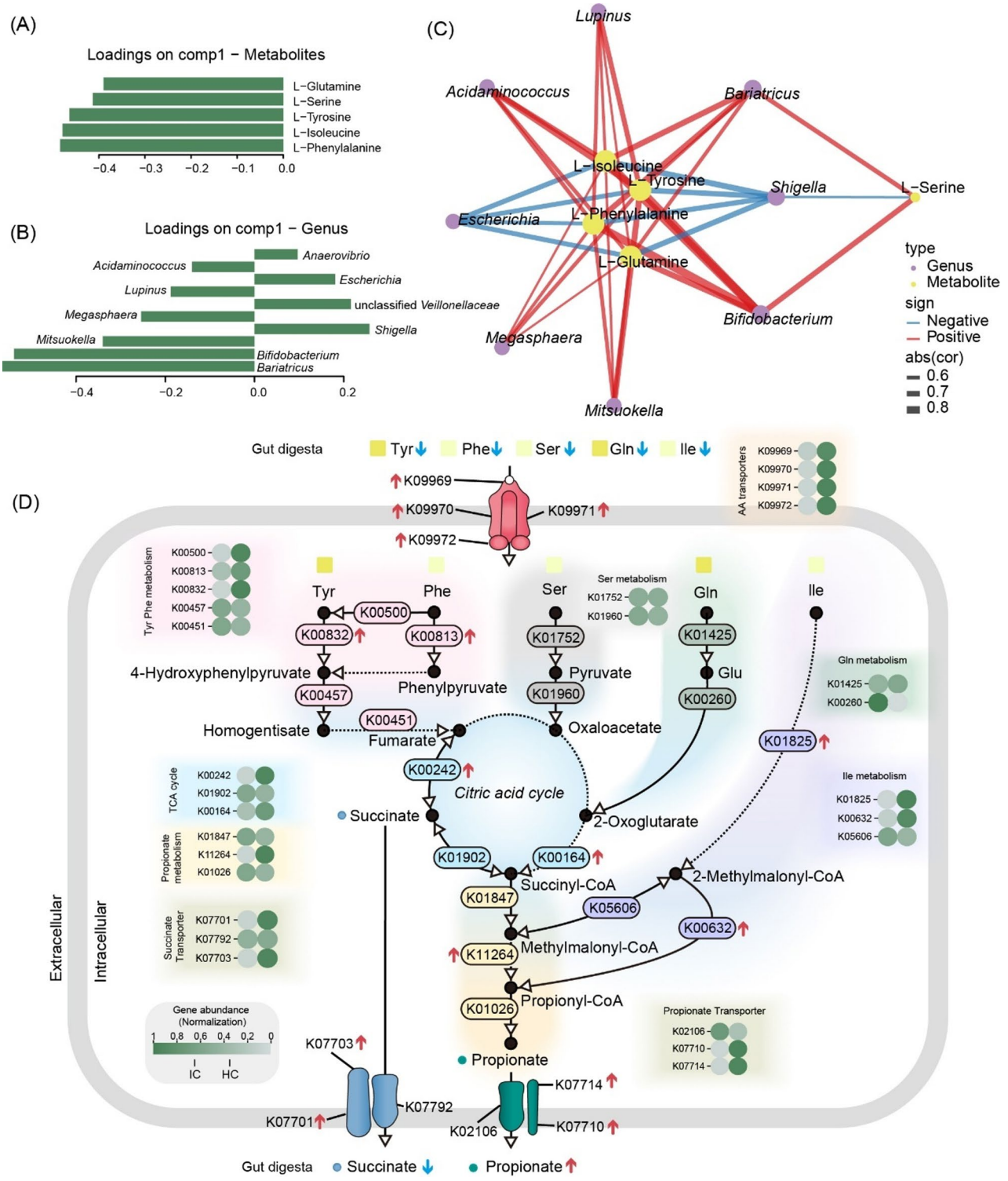

Fig. 2 Associations between gut microbial genera, amino acids, and microbial genes involved in amino acid transport and metabolism. (**A**) Loadings of metabolites on the first component (comp1) derived from sparse partial least squares (sPLS) analysis. (**B**) Loadings of bacterial genera on comp1 from the same sPLS model. (**C**) Correlation network constructed based on sPLS-selected metabolites and genera. Nodes represent metabolites (yellow) and bacterial genera (purple), and edges indicate significant correlations between metabolites and genera. Red and blue edges denote positive and negative correlations, respectively, with edge width proportional to the absolute correlation coefficient. (**D**) Proposed microbial metabolic and transport pathways linking altered amino acid profiles to central carbon metabolism and propionate production. Upward and downward arrows indicate significantly (FDR < 0.05) increased or decreased metabolites or genes, respectively

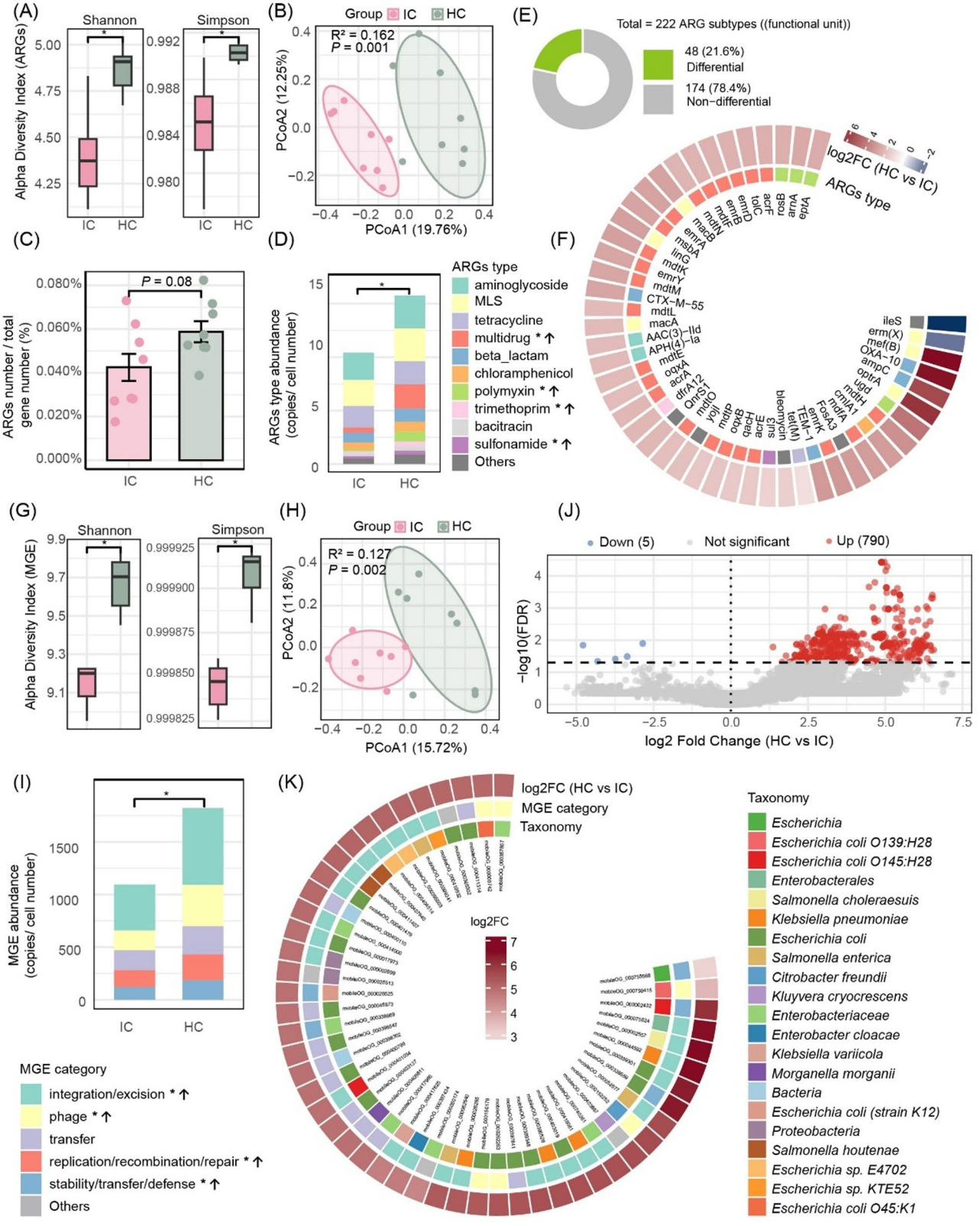

Fig. 3 (See legend on next page.)

(See figure on previous page.)

Fig. 3 Comparative analysis of antibiotic resistance genes (ARGs) and mobile genetic elements (MGEs) between IC and HC groups. (**A**) Boxplots of Shannon and Simpson alpha diversity indices for ARGs. (**B**) Principal coordinate analysis (PCoA) based on Jaccard distances of ARGs. (**C**) Barplot showing percentage of ARGs relative to the total number of genes. (**D**) Stacked bar plot of ARG types classified by antibiotic category. (**E**) Overview of differential ARG subtypes between groups. Among a total of 222 ARG subtypes (functional units), the proportion of differential and non-differential ARGs is shown. (**F**) Circular heatmap of differential ARG subtypes between HC and IC groups. The outer ring represents log2 fold changes (HC vs. IC), while inner annotations indicate ARG types. (**G**) Boxplots of Shannon and Simpson alpha diversity indices for MGEs. (**H**) Principal coordinate analysis (PCoA) based on Jaccard distances of MGEs. (**I**) Stacked bar plot showing the composition of MGEs classified by functional category. (**J**) Volcano plot of differential MGE features between HC and IC groups. The x-axis represents log2 fold changes, and the y-axis shows –log10(FDR). (**K**) Circular visualization of top 50 differential MGEs integrating log2 fold changes (outer ring), MGE functional categories (middle ring), and taxonomic affiliations (inner ring)

significantly higher ARG diversity in the HC group, as indicated by both Shannon and Simpson indices (Fig. 3A). Consistently, beta diversity analysis based on Jaccard distances showed a clear separation of ARG profiles between groups (R^2 = 0.162, P = 0.001; Fig. 3B). In addition to compositional shifts, the overall ARG burden tended to be in the HC group. Specifically, the relative abundance of ARGs—calculated as the proportion of ARGs relative to the total gene count—showed an increasing trend following casein hydrolysate supplementation (P = 0.08; Fig. 3C). Stratification of ARGs by resistance category further revealed enrichment of genes associated with multidrug resistance, as well as resistance to polymyxins, sulfonamides, and trimethoprim in the HC group (Fig. 3D). At the subtype level, among a total of 222 detected ARG subtypes (functional units), 48 subtypes were identified as differentially abundant between groups based on an FDR threshold of < 0.05 (Fig. 3E). Of these, 46 ARG subtypes exhibited significantly higher abundances in the HC group, whereas only two ARGs—*ileS* and *erm(X)*—were reduced relative to the IC group (Fig. 3F), indicating a pronounced shift of the resistome toward increased abundance following casein hydrolysate supplementation.

Given the close relationship between antibiotic resistance dissemination and MGEs, we further examined MGE profiles across groups. Both diversities of MGEs were significantly altered in the HC group, as indicated by increased Shannon and Simpson indices (Fig. 3G) and clear separation of MGE profiles based on Jaccard distances (Fig. 3H). Functional classification revealed that four major MGE categories—integration/excision, transposition, phage-associated elements, and recombination/repair functions—were significantly enriched following casein hydrolysate supplementation (Fig. 3I). Differential analysis further revealed a pronounced shift in MGE abundance, with 790 MGE features significantly enriched in the HC group, whereas only five MGEs were reduced relative to the IC group, as visualized in the volcano plot based on an FDR threshold of < 0.05 (Fig. 3J). Moreover, the majority of the top 50 differentially abundant MGEs were taxonomically assigned to *Escherichia coli* and other members of the Enterobacteriaceae family (Fig. 3K), suggesting an increased prevalence of mobile genetic elements within these taxa. Together, these results indicate that casein hydrolysate supplementation is associated with concurrent expansion of the resistome and mobilome, potentially increasing the capacity for horizontal gene transfer within the gut microbiome.

Microbiome-metabolome integration revealed close associations between amino acids and antibiotic resistance genes

To investigate whether alterations in amino acid metabolism were associated with changes in the resistome and mobilome, we performed integrative analyses combining amino acid–related metabolites with ARG and MGE profiles. Procrustes analysis revealed significant concordance between the overall ordination structures of amino acids-related metabolites and ARG profiles (r = 0.62, P = 0.002), as well as MGEs (r = 0.64, P = 0.0014), indicating a close correspondence between metabolic variation and resistome/mobilome configurations across samples (Fig. 4A).

Complementing the Procrustes analysis, Mantel correlation analysis further demonstrated significant associations among amino acids-related metabolites, amino acid–related functional genes, ARGs, and MGEs, as well as with microbial alpha diversity and taxonomic composition (Fig. 4B). These correlations were predominantly positive. Notably, ARGs and MGEs exhibited a strong positive association with each other (r = 0.81, P < 0.001), and both were positively correlated with amino acid profiles, with correlation coefficients of r = 0.32 for ARGs and r = 0.31 for MGEs (Fig. 4B). Together, these results indicate that shifts in amino acid metabolism occurred in parallel with coordinated changes in microbial community structure and resistance-related genetic features.

To resolve these relationships at finer resolution, we examined correlations between individual amino acids and ARG categories. Several amino acids and their metabolic derivatives, including glutamine, tyrosine, phenylalanine, serine, isoleucine, kynurenic acid, and related compounds, exhibited significant associations with multiple ARG classes, particularly multidrug and β-lactam resistance categories (Fig. 4C).

Finally, correlation analysis at the ARG subtype level revealed distinct association patterns between amino acids and their metabolic derivatives (Fig. 4D). Core amino acids, including tyrosine and glutamine, were

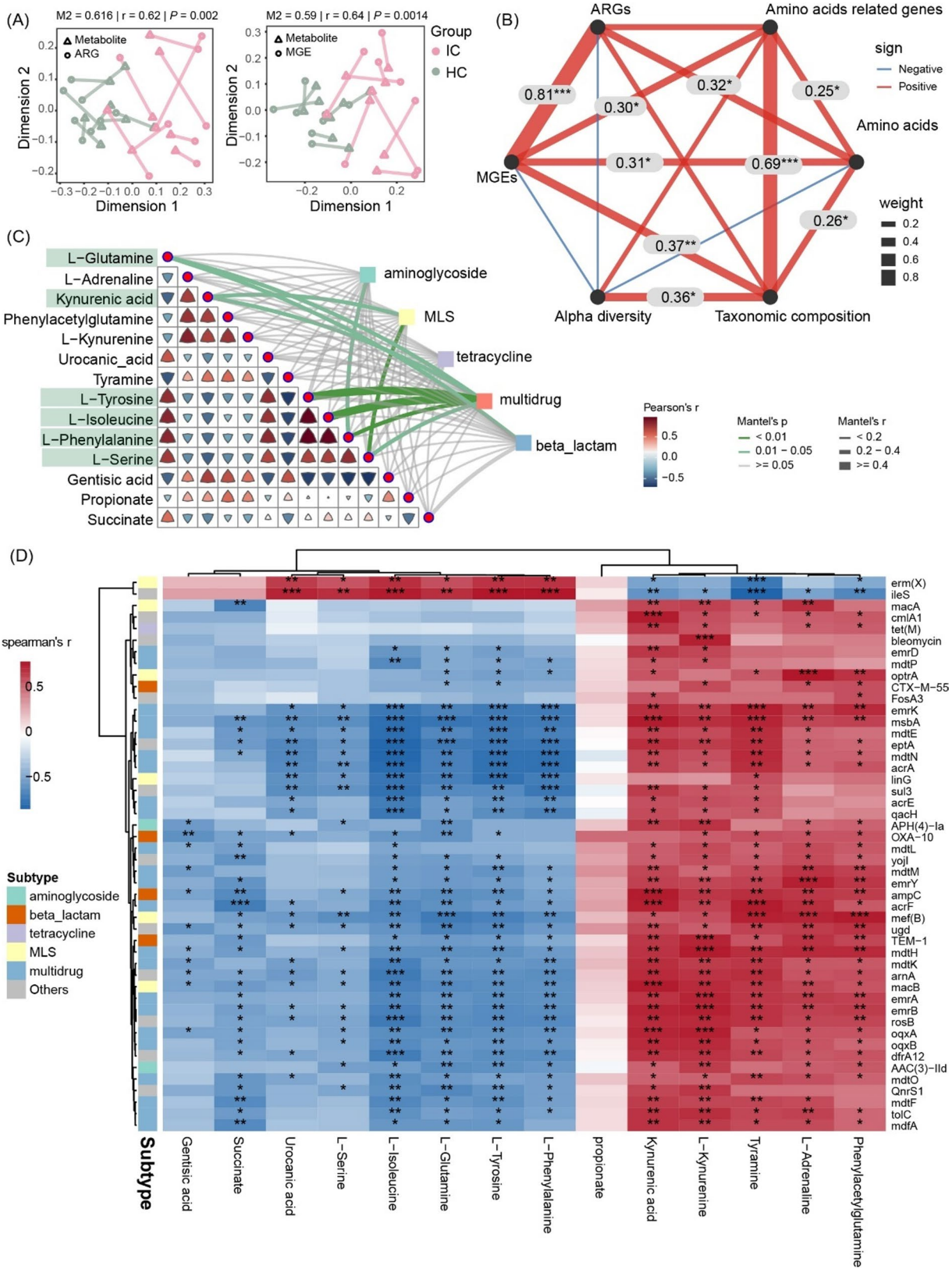

Fig. 4 (See legend on next page.)

(See figure on previous page.)

Fig. 4 Integrated correlation analysis of amino acid-related metabolites, resistome and mobilome. (**A**) Procrustes analysis comparing ordination structures of amino acids and related metabolites with those of ARGs (left) and MGEs (right). Points represent individual samples, triangles indicate metabolites, and circles indicate ARG or MGE profiles. Lines connect corresponding samples across datasets. (**B**) Mantel correlation network summarizing pairwise associations among amino acids, amino acid–related genes, ARGs, MGEs, alpha diversity, and taxonomic composition. Edge color indicates correlation direction (red, positive; blue, negative), edge width represents correlation strength. (**C**) Correlation network linking individual amino acids and metabolites to ARG categories. Nodes represent amino acids/metabolites (left) and ARG classes (right). Edge color reflects Pearson's correlation coefficients, while edge thickness indicates Mantel's r. (**D**) Heatmap of Spearman correlations between differential amino acids/metabolites and differential ARG subtypes. Colors represent correlation coefficients, and asterisks denote significance levels

predominantly negatively correlated with ARG subtypes, whereas amino acid–derived metabolites and downstream fermentation products such as tyramine and kynurenic acid exhibited mainly positive correlations with ARGs, indicating divergent association trends between substrate amino acids and their metabolic outputs. Together, these integrative analyses indicate that alterations in amino acid metabolism are closely associated with coordinated changes in the resistome and mobilome, highlighting a tight coupling between microbial metabolic activity and antibiotic resistance gene profiles in response to casein hydrolysate supplementation.

MAG-based analysis showed microbial taxa co-harboring amino acid metabolism and antibiotic resistance genes

To further identify microorganisms with genomic potential for both amino acid utilization and antibiotic resistance, 274 high-quality MAGs were reconstructed from cecal metagenomics datasets. A comprehensive phylogenetic tree was generated to illustrate the taxonomic distribution of these MAGs, with annotations provided at the phylum level (Fig. 5). Analysis of functional gene distribution across the MAGs revealed that while the majority of bins harbored genomic potential for the transport and metabolism of amino acids—specifically tyrosine, glutamine, phenylalanine, serine, and isoleucine—only a subset contained genes associated with SCFA transport or antibiotic resistance (Fig. 6). Notably, bin54 emerged as a uniquely enriched MAG, distinguished by its simultaneous possession of genes involved in amino acid transport and metabolism, SCFA transport, and ARGs. It also contained the highest number of MGEs among all bins. These features suggest that bin54 may serve as a key microbial node linking nutrient processing with the mobilization of resistance genes in the cecal microbiome.

Figure 6A summarizes all MAGs that concurrently encoded genes related to amino acid transport and metabolism, antibiotic resistance, and MGEs, along with their corresponding taxonomic classifications. Notable examples include bin121 (*Campylobacter sp945873855*), bin54 (*Escherichia fergusonii*), bin46 (*Limosilactobacillus mucosae*), bin58 (*Streptococcus alactolyticus*), and bin142 (*Bifidobacterium thermophilum*), representing microbial taxa with multifaceted functional potential in the cecal microbiome.

The contig-level distribution of relevant genes within each bin was analyzed to further explore the genomic architecture underlying this co-occurrence. Notably, only bin54 and bin142 contained contigs where amino acid transport/metabolism genes, ARGs, and MGEs were co-located in close proximity on the same scaffold (Fig. 6B and C). Detailed gene cluster analysis revealed physical co-localization of amino acid transport and metabolism genes (e.g., *ABC.P.A.A*, *ABC.P.A.P*, *aapP*, *aapM*, *aapQ*), antibiotic resistance genes (e.g., *tgpA*, *acrF*, *acrA*, *acrB*, *mdfA*), and MGEs (e.g., *xer*, *PSLT501*) on the same contigs in representative MAGs (Fig. 6B and C). Among these, bin54_node_2637 emerged as the most functionally convergent contig, with genes related to amino acid uptake, resistance, and mobility densely clustered. This genomic arrangement suggests a potential functional coupling between nutrient metabolism and resistance gene dissemination within individual microbial genomes.

Discussion

In this study, a pig model was used to examine the impact of casein hydrolysate on microbial amino acid metabolism and the gut resistome. Casein hydrolysate supplementation was associated with pronounced alterations in luminal amino acid availability, which were closely linked to microbial amino acid transport and metabolic pathways. Notably, the increased abundance of ARGs and MGEs exhibited strong associations with both microbiome composition and amino acid profiles. Furthermore, metagenome-assembled genome analysis revealed the co-occurrence of resistome components with genes involved in amino acid transport and metabolism, supporting a potential mechanistic coupling between microbial nutrient utilization and resistance-related genetic features.

Casein hydrolysate reshapes amino acid availability in the gut and may elicit coordinated adaptive responses in both the host and the gut microbiota. First, casein hydrolysate supplementation significantly reduced the concentrations of several amino acids in the cecal digesta, including tyrosine and glutamine, despite the higher levels of free amino acids present in the diet [6]. This apparent discrepancy suggests that dietary amino acids derived from casein hydrolysate were more efficiently utilized along the gastrointestinal tract rather than accumulating in the distal gut. Consistent with this interpretation,

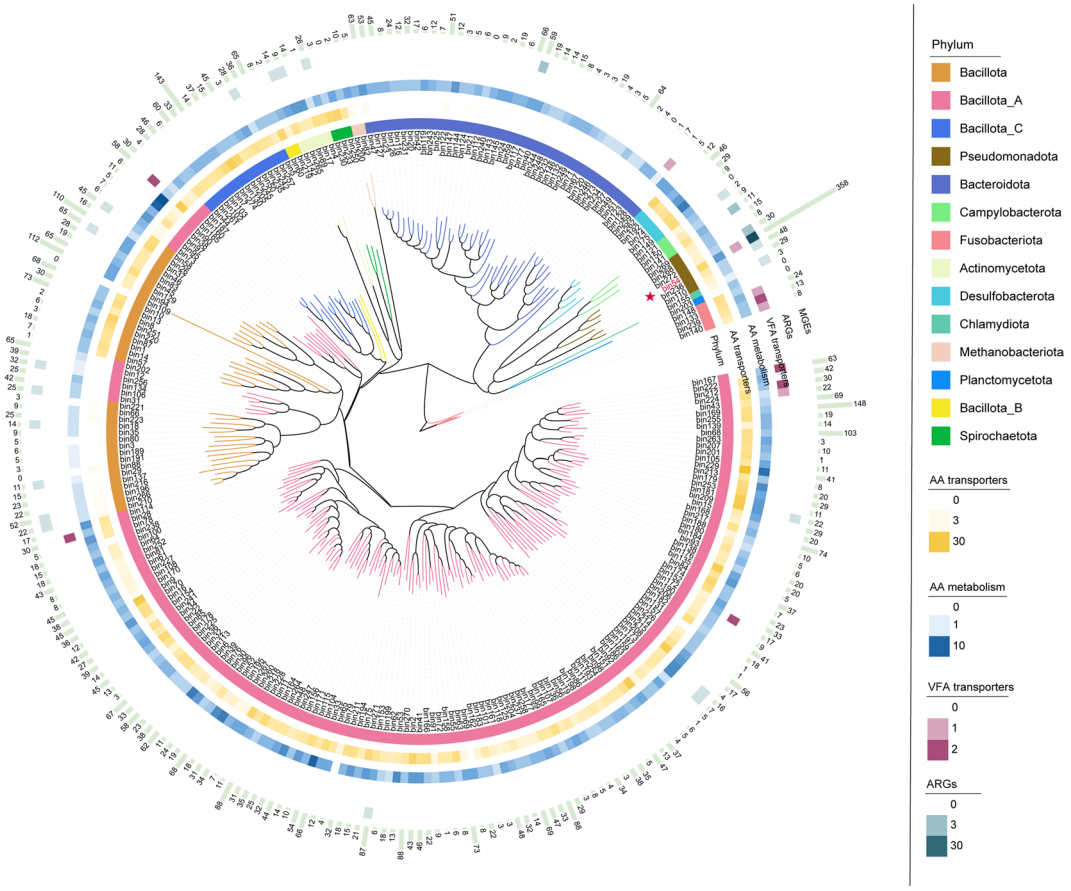

Fig. 5 Phylogenetic tree of 274 metagenome-assembled genomes (MAGs). From innermost to outermost, the concentric heatmap rings represent microbial taxonomy at the phylum level, amino acid (AA) transporters, AA metabolism genes, VFA transporters, ARGs, and MGEs

previous peptidomic studies have shown that casein hydrolysate accelerates gastrointestinal transit and generates smaller and more homogeneous peptide profiles compared with intact casein, resulting in earlier and more efficient amino acid absorption in the upper intestine and reduced nitrogen delivery to the distal gut [25]. In parallel with altered luminal amino acid availability, host amino acid absorption capacity is enhanced, as evidenced by the upregulation of amino acid transporters in the gastric corpus following casein hydrolysate supplementation [6]. Extending these findings, metagenomics analysis in the present study further revealed a significant enrichment of microbial genes encoding ATP-binding cassette (ABC)–type L-amino acid transporters in the casein hydrolysate group. These high-affinity, ATP-dependent transport systems enable bacteria to efficiently scavenge amino acids and small peptides from the surrounding environment [30, 31]. Importantly, a recent finding suggests that casein-derived oligopeptides do not merely serve as microbial nutrient substrates but can also function as regulatory effectors that induce the expression of peptide and amino acid transport systems and associated metabolic pathways [26]. Such peptide-mediated regulation may prime microbial nutrient uptake and metabolic activity, thereby conferring growth and environmental fitness advantages under competitive gut conditions. Taken together, these observations suggest that casein hydrolysate may induce coordinated host–microbiota adaptation to an amino acid– and peptide-enriched luminal environment.

The gastrointestinal tract represents a major reservoir and transmission hub for ARGs [27], while MGEs, such as plasmids and transposons, facilitate their horizontal dissemination across microbial communities [15]. Emerging evidence indicates that microbial metabolic states, particularly those shaped by nutrient availability, play an important role in modulating antibiotic resistance [28]. Notably, elevated ARGs and MGEs in present study were negatively correlated with several amino acids, including tyrosine and glutamine, suggesting that amino acid metabolism may be linked to resistome dynamics. This observation is consistent with previous reports showing that fluctuations in amino acid availability are associated with temporal variations in ARG abundance in pigs [29]. More specifically, individual amino acids appear to exert distinct and sometimes context-dependent effects

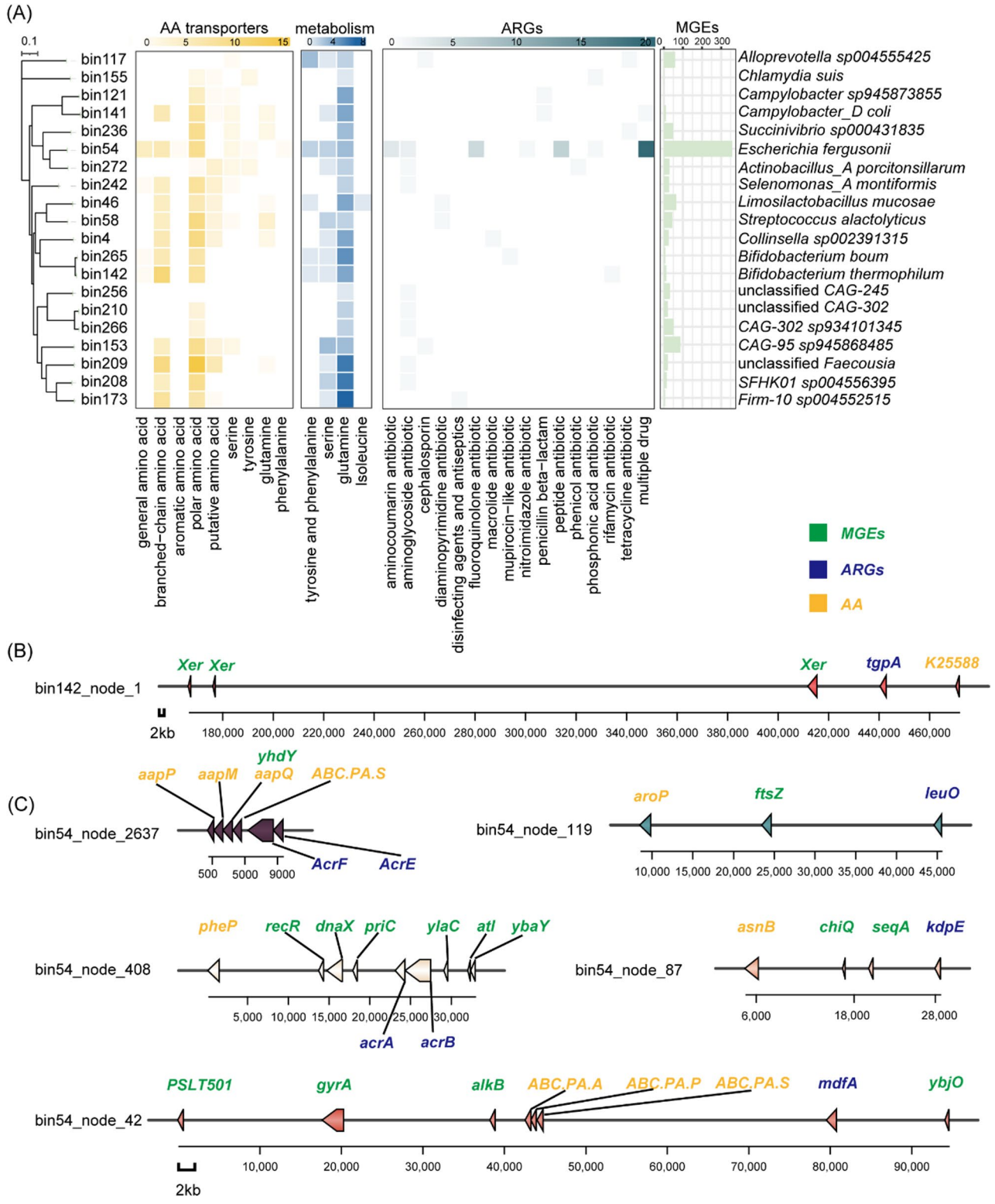

Fig. 6 Co-localization of AA transport/metabolism genes, ARGs, and MGEs on the same contigs. (**A**) Heatmap showing the distribution of AA transporters, AA metabolism genes, ARGs, and MGEs across MAGs that simultaneously harbor all three categories of functional genes. The right panel indicates the taxonomic annotation of each MAG. Gene clusters of representative contig from bin142 (**B**) and bin54 (**C**), showing co-localized ARGs, MGEs, and AA-associated genes. Colored arrows indicate different gene categories: AA-related genes (orange), ARGs (blue), MGEs (green)

on the gut resistome. For example, supplementation with 0.2% methionine has been associated with a reduced abundance of ARGs in the intestinal microbiota of sows [30]. Beyond changes in ARG prevalence at the community level, mechanistic studies further demonstrated that L-methionine supplementation can restore tigecycline sensitivity in *tet(X)*-positive *Escherichia coli* by reprogramming bacterial metabolism and epigenetic regulation, thereby attenuating resistance phenotypes without necessarily eliminating resistance genes [31]. Similarly, glutamine has been implicated as a key metabolic modulator linking amino acid utilization to antibiotic susceptibility. Glutamine supplementation has been shown to enhance central carbon metabolism, including activation of the tricarboxylic acid cycle and increased NADH production, which elevates the proton-motive force and promotes antibiotic uptake in resistant bacteria [32]. These findings further support the notion that amino acid-driven metabolic reprogramming can influence antibiotic resistance primarily at the functional level, and that the impact of individual amino acids on the resistome is highly dependent on metabolic context and microbial physiological state.

Beyond amino acid availability itself, the downstream metabolic fate of amino acids and their fermentation-derived products may also be closely linked to gut resistome dynamics. In the casein hydrolysate group, succinate levels were reduced whereas propionate levels were increased, indicating a redirection of microbial metabolic flux toward propionate production [33]. Accumulating evidence suggests that propionate is closely associated with the gut resistome, as propionate levels have been linked to both the abundance and temporal oscillation of specific ARGs and MGEs, highlighting short-chain fatty acids as important metabolic intermediates connecting microbial activity with resistance-related genetic features [34] In parallel, tryptophan metabolism was markedly altered following casein hydrolysate supplementation. Metabolites within the kynurenine pathway, including kynurenine and kynurenic acid, were significantly increased, indicating enhanced utilization and transformation of tryptophan. Supporting a link between tryptophan metabolism and resistome responses, previous studies have shown that antibiotic interventions suppressing microbial activity are accompanied by reductions in tryptophan-related metabolites alongside pronounced changes in ARG abundance [35]. Meanwhile, the indole-derived tryptophan metabolite indole-3-carboxaldehyde was decreased, suggesting a redistribution of tryptophan metabolism across distinct downstream branches. Consistently, another indole-derived metabolite, indole-3-acetic acid, has been reported to be closely associated with ARG variation in different ecological contexts [36]. Together, these findings indicate that both central fermentation products and branch-specific tryptophan-derived metabolites are tightly associated with gut resistome dynamics.

Antibiotic resistance genes and amino acid metabolism–related genes appear to be positionally associated within bacterial genomes. In the present study, metagenome assembly and binning were employed to examine the genomic distribution of genes involved in amino acid transport and metabolism, VFA transporters, ARGs, and MGEs. Notably, genes related to amino acid transport, ARGs, and MGEs were co-localized on the same contigs in *Escherichia fergusonii* and *Bifidobacterium thermophilum*, indicating a tight genomic coupling between nutrient acquisition and resistance-related functions. Consistent with this observation, previous studies have reported a significant co-occurrence of ARGs and metabolic genes—particularly those involved in carbohydrate and amino acid metabolism—in *Escherichia coli*, where these genes are frequently co-localized on the same plasmids [37]. The presence of metabolic genes on conjugative plasmids is thought to facilitate the maintenance and dissemination of ARGs by mitigating the fitness costs associated with plasmid carriage and enhancing bacterial survival under antibiotic pressure. Beyond directly encoding resistance determinants, MGEs can also indirectly reshape host metabolism by reallocating intracellular resources and altering nutrient uptake and metabolic fluxes, including pathways related to amino acid acquisition and utilization, even in the absence of MGE-encoded metabolic enzymes [38]. Such MGE-associated metabolic reprogramming has been shown to influence bacterial fitness and interspecies interactions, with consequences for community structure and function. Moreover, amino acid and peptide transporters in *Staphylococcus aureus* have been shown to influence bacterial survival, virulence, and antibiotic resistance, underscoring membrane transport systems as potential targets for attenuating resistance phenotypes [39]. Together, these findings suggest that *E. fergusonii* exhibits a similar genomic organization, in which amino acid transporters are not only highly represented but also frequently co-localized with ARGs and MGEs. This genomic arrangement highlights a potential adaptive strategy whereby enhanced nutrient acquisition capacity is coupled to resistance determinants, thereby promoting bacterial fitness and facilitating the persistence and dissemination of antibiotic resistance in the gut environment.

Several limitations of the present study should be acknowledged. First, in line with the primary research objective, the experimental design focused on comparing casein hydrolysate with intact casein, without including an additional normal-protein control group. While this design allowed us to specifically evaluate the effects of protein hydrolysis, it precluded a broader assessment

of how different protein sources or baseline protein conditions might influence amino acid metabolism and resistome profiles. Second, the associations observed between amino acid metabolism, including downstream fermentation products, and antibiotic resistance genes were based on correlation analyses. Therefore, causal relationships cannot be inferred from the current data. Future studies employing targeted microbial manipulation, isotope tracing, or controlled intervention experiments will be required to elucidate the mechanistic links between amino acid metabolic pathways and resistome dynamics.

Overall, casein hydrolysate supplementation altered amino acid metabolism in the cecum by reshaping the gut microbiota's metagenome-predicted capacity for amino acid transport and utilization. These metabolic changes were accompanied by coordinated alterations in the gut resistome. Together, our findings highlight a close association between microbial amino acid metabolism and antibiotic resistance within the gut ecosystem.

Supplementary Information

The online version contains supplementary material available at https://doi.org/10.1186/s42523-026-00542-z.

Supplementary Material 1

Author contributions

CL.M. and W.Z. designed this project. Z.L. performed the study, analyzed the data, and wrote the paper. J.S. and H.W. conducted the animal experiment. W.Z., J.Z and CL.M. edited and revised the paper. CM. M assisted in organizing sample analysis and measuring the concentrations of SCFA and organic acids. J.G. contributed to data analysis. All authors have read and approved the final manuscript.

Funding

The study was supported by National Natural Science Foundation of China (32030104, 31430082) and Norway International Collaborative Project SiNorAMR.

Data availability

The raw reads from metagenomics sequencing have been deposited at NCBI Sequence Read Archive (SRA) database with the BioProject accession number PRJNA1264679 (Sus scrofa, TaxID: 1510822). The raw metabolomics data generated in this study have been deposited in the OMIX repository at the National Genomics Data Center (NGDC) under accession number OMIX011452.

Declarations

Competing interests

The authors declare no competing interests.

Received: 11 July 2025 / Accepted: 1 March 2026
Published online: 01 May 2026

References

1. Zhao, Jianfei X, Zhang H, Liu MA, Brown SQ. Dietary protein and gut microbiota composition and function. Curr Protein Pept Sci. 2019;20:145–54. https://doi.org/10.2174/1389203719666180514145437.
2. Yang Z, Shengfa F, Liao. Physiological effects of dietary amino acids on gut health and functions of swine. Front veterinary Sci. 2019;6:169. https://doi.org/10.3389/fvets.2019.00169.
3. Shen J, Mu C, Wang H, Huang Z, Yu K, Erwin G, Zoetendal WZ. Stimulation of gastric transit function driven by hydrolyzed casein increases small intestinal carbohydrate availability and its microbial metabolism. Mol Nutr Food Res. 2020;64:2000250. https://doi.org/10.1002/mnfr.202000250.
4. Liu S, Zhu H, Ren Y, Wu WFH, Wu H, Huang Z, Zhu W. A hydrolyzed casein diet promotes Ngn3 controlling enteroendocrine cell differentiation to increase gastrointestinal motility in mice. Food Funct. 2024;15:1237–49. https://doi.org/10.1039/d3fo04152b.
5. Jing Y, Mu C, Wang H, Shen J, Zoetendal EG, Zhu W. Amino acid utilization allows intestinal dominance of Lactobacillus amylovorus. ISME J. 2022;16:2491–502. https://doi.org/10.1038/s41396-022-01287-8.
6. Mu C, Shen J, Wang H, Yu K, Su Y, Zhu W. Casein Hydrolysate Enhances Upper Gastrointestinal Chemosensing and Gastric Acid Secretion in Pigs. J Agric Food Chem. 2025;73:7857–66. https://doi.org/10.1021/acs.jafc.5c01141.
7. Dai Z, Wu Z, Zhu W, Wu G. Amino Acids in Microbial Metabolism and Function. Adv Exp Med Biol. 2022;1354:127–43. https://doi.org/10.1007/978-3-030-85686-1_7.
8. Neis, Evelien PJG, Cornelis HC, Dejong, Sander S, Rensen. The role of microbial amino acid metabolism in host metabolism. Nutrients. 2015;7:2930–46. https://doi.org/10.3390/nu7042930.
9. Liu, Ziyu C, Mu WZ. Metagenomics-based inference of microbial metabolism towards neuroactive amino acids and the response to antibiotics in piglet colon. Amino Acids. 2023;55:1333–47. https://doi.org/10.1007/s00726-023-03311-3.
10. Perry JA, Westman EL, Wright GD. The antibiotic resistome: what's new? Curr Opin Microbiol. 2014;21:45–50. https://doi.org/10.1016/j.mib.2014.09.002.
11. Kim DW, Cha CJ. Antibiotic resistome from the One-Health perspective: understanding and controlling antimicrobial resistance transmission. Experimental Mol Med. 2021;53:301–9. https://doi.org/10.1038/s12276-021-00569-z.
12. McInnes RS, McCallum GE, Lamberte LE, van Schaik W. Horizontal transfer of antibiotic resistance genes in the human gut microbiome. Curr Opin Microbiol. 2020;53:35–43. https://doi.org/10.1016/j.mib.2020.02.002.
13. Schjørring S, Karen AK. Assessment of bacterial antibiotic resistance transfer in the gut. Int J Microbiol. 2011;2011:312956.
14. Jian Z, Zeng L, Xu T, Sun S, Yan S, Yang L, Huang Y, Jia J, Dou T. Antibiotic resistance genes in bacteria: Occurrence, spread, and control. J Basic Microbiol. 2021;61:1049–70. https://doi.org/10.1002/jobm.202100201.
15. Partridge, Sally R, Stephen M, Kwong N, Firth, Slade OJ. Mobile genetic elements associated with antimicrobial resistance. Clin Microbiol Rev. 2018;31. https://doi.org/10.1128/CMR.00088-17
16. Broaders E, Gahan CGM, Julian RM. Mobile genetic elements of the human gastrointestinal tract: potential for spread of antibiotic resistance genes. Gut Microbes. 2013;4:271–80. https://doi.org/10.4161/gmic.24627.
17. Kim Y, Leung MHY, Kwok W, Fournie G, Li J, Lee PKH, Pfeiffer DU. Antibiotic resistance gene sharing networks and the effect of dietary nutritional content on the canine and feline gut resistome. Anim Microbiome. 2020;2:4. https://doi.org/10.1186/s42523-020-0022-2.
18. Oliver A, Xue Z, Villanueva YT, Durbin-Johnson B, Alkan Z, Taft DH, Liu J, Korf I, Kevin D, Laugero, Charles B, Stephensen. Association of diet and antimicrobial resistance in healthy US adults. MBio. 2022;13:e00101–00122.
19. Freiberg JA, Valeria M, Reyes Ruiz BD, Gimza CC, Murdoch ER, Green, Jacob M, Curry JE, Cassat, Eric PS. Restriction of arginine induces antibiotic tolerance in Staphylococcus aureus. Nat Commun. 2024;15:6734.
20. Liu, Yuan K, Yang H, Zhang Y, Jia ZW. Combating antibiotic tolerance through activating bacterial metabolism. Front Microbiol. 2020;11:577564.
21. Bolger AM, Lohse M, Bjoern Usadel. Trimmomatic: a flexible trimmer for Illumina sequence data. Bioinformatics. 2014;30:2114–20.
22. Hyatt D, Chen G-L, LoCascio PF, Land ML, Larimer FW, Loren JH. Prodigal: prokaryotic gene recognition and translation initiation site identification. BMC Bioinformatics. 2010;11:1–11. https://doi.org/10.1186/1471-2105-11-119.
23. Fu L, Niu B, Zhu Z, Wu S, Li W. CD-HIT: accelerated for clustering the next-generation sequencing data. Bioinformatics. 2012;28:3150–2. https://doi.org/10.1093/bioinformatics/bts565.
24. Patro R, Duggal G, Love MI, Irizarry RA, Carl Kingsford. Salmon provides fast and bias-aware quantification of transcript expression. Nat Methods. 2017;14:417–9. https://doi.org/10.1038/nmeth.4197.

25. Jiménez-Barrios P, Sánchez-Rivera L, Martínez-Maqueda D, Le Gouar Y, Didier D, Miralles B, Recio IJ. Peptidomic characterization and amino acid availability after intake of casein vs. a casein hydrolysate in a pig model. 2023;15:1065.
26. Hao X, Song X, Ren J, Dudu OE, Jiang J, Zeng J, Song Wang, et al. A novel peptide derived from casein hydrolysates as a growth factor for lactobacillus delbrueckii subsp. bulgaricus sp1.1. 2025;197:6120–42.
27. Carlet J. The gut is the epicentre of antibiotic resistance. Antimicrob Resist Infect control. 2012;1:1–7.
28. Xu J, Wang H, Xu R, Li Q, Su Y, Liu J, Weiyun Zhu. The diurnal fluctuation of colonic antibiotic resistome is correlated with nutrient substrates in a pig model. Sci Total Environ. 2023;891:164692.
29. Wang, Hongyu Y, Li J, You N, Feng D, Wang Y, Su XF. Diurnal oscillations of amino acids dynamically associate with microbiota and resistome in the colon of pigs. Anim Microbiome. 2025;7:26. https://doi.org/10.1186/s42523-025-00393-0.
30. Cai S, Yang Y, Zeng X, Zhu Z, Wang F, Zhang S, Chen F, Cai C, Zeng X, Shiyan Qiao. Methionine influences the profile of intestinal antibiotic resistome through inhibiting the growth of Escherichia coli. Sci Total Environ. 2023;899:165610.
31. Fang D, Xu T, Li F, Sun Y, Yin JSY, Zhang H, Wang Z, Yuan Liu. Methionine-driven methylation modification overcomes plasmid-mediated high-level tigecycline resistance. Nat Commun. 2025;16:417. https://doi.org/10.1038/s41467-024-55791-w.
32. Yong Y, Zhou Y, Liu K, Liu G, Wu L, Fang B. Exogenous citrulline and glutamine contribute to reverse the resistance of Salmonella to apramycin. Front Microbiol. 2021;12:759170.
33. Wang Z, Kang S, Wu Z, Liu X, Zhang X, Wu Y, Wen Y, Zhou X, Zhang G, Junjun Wang. Muribaculum intestinale restricts Salmonella Typhimurium colonization by converting succinate to propionate. ISME J. 2025;19:wraf069. https://doi.org/10.1093/ismejo/wraf069.
34. Zhang Y, Zhang S, Yuan Y, Li Y, Zhu R, Yang Y, Xing S, Wang Y, Wu Y, Liao X. Metagenomic assembly reveals the circadian oscillations of the microbiome and antibiotic resistance genes in a model of laying hens. Sci Total Environ. 2022;836:155692.
35. Oladele P, Wickware CL, Trachsel J, Looft T, Johnson TA. In-feed bacitracin methylene disalicylate alters microbiota function and increases antibiotic resistance in a dose-dependent manner. bioRxiv. 2025:2025.2002.2016.638580.
36. Chen P, Yu K, Yang K, Zhang D, Li P, He Y. Indole-3-acetic acid-mediated root exudates as potential inhibitors of antibiotic resistance genes in the rhizosphere microbiome: mechanistic insights into microbial community assembly and resistome dissemination. Bioresour Technol. 2025;133191.
37. Palomino A, Gewurz D, DeVine L, Zajmi U, Moralez J, Abu-Rumman F, Smith RP, Allison JL. Metabolic genes on conjugative plasmids are highly prevalent in Escherichia coli and can protect against antibiotic treatment. ISME J. 2023;17:151–62.
38. Bisesi AT, Carlson RP, Cotner L, Harcombe WR. Metabolic remodeling of microorganisms by mobile genetic elements alters mutualistic community composition. mSystems. 2025;10:e00144-25.
39. Zeden M, Suzan Órla, Burke M, Vallely C, Fingleton JP, O'Gara. Exploring amino acid and peptide transporters as therapeutic targets to attenuate virulence and antibiotic resistance in Staphylococcus aureus. PLoS Pathog. 2021;17:e1009093.

Publisher's note